Electronic Supplementary Material (ESI) for Nanoscale.

A Direct Z-Scheme PtS_2/Arsenene van der Waals Heterostructure with High Photocatalytic Water Splitting Efficiency

Kai Ren[a,b], Wencheng Tang[a,*], Minglei Sun[a], Yongqing Cai[c], Yuan Cheng[b] and Gang Zhang[b,*]

[a] School of Mechanical Engineering, Southeast University, Nanjing, Jiangsu 211189, China
[b] Institute of High Performance Computing, A*STAR, Singapore 138632, Singapore
[c] Institute of Applied Physics and Materials Engineering, University of Macau, Taipa, Macau, China
* E-mail address: 101000185@seu.edu.cn (Wencheng Tang); zhangg@ihpc.a-star.edu.sg (G. Zhang)

1. Effect of SOC

The band structures of the PtS_2/Are vdW heterostructure calculated by PBE functional with or without spin-orbit coupling (SOC) are shown in Fig. S1. It is clear that SOC has negligible effect on the band gap and band alignment of the PtS_2/Are vdW heterostructure.

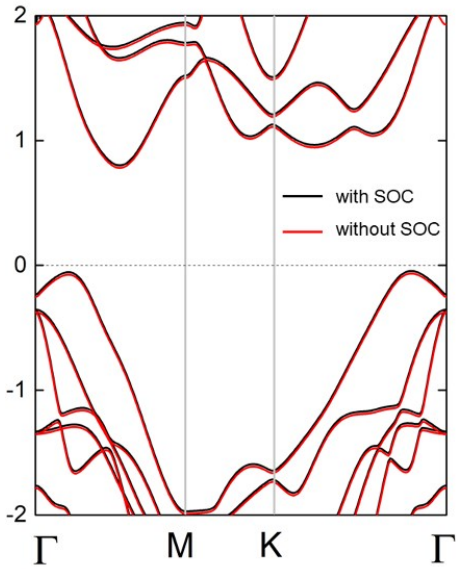

Fig. S1. The band structure of the PtS_2/Are vdW heterostructure with and without spin-orbit coupling calculated by PBE calculations.

2. The different stacking configurations

When the vertical heterostructure was constructed by PtS_2 and Are monolayers, 6 representative stacking configurations, stacking-A, stacking-B, stacking-C, stacking-D, stacking-E and stacking-F, are considered, as shown in Fig. S2. As for stacking-A configuration, the lower As atoms of the Arsenene (Are) are located on the top of Pt atoms of the PtS_2, while the upper As atoms are on the top of the upper S atoms. For stacking-B configuration, the lower As atoms of the Are still locate on the top of Pt atoms of the PtS_2, but the upper As atoms are on the top of lower S atoms. Putting the upper As atoms on the top of the upper S atoms and the lower As atoms on the top of the lower S atoms will obtain the stacking-C configuration. And for stacking-D configuration, we put the upper As atoms on the top of Pt atoms and the lower As atoms on the top of the upper S atoms. The stacking-E configuration is constructed by locating the upper As atoms on the top of Pt atoms and the lower As atoms on the lower S atoms. As for stacking-F configuration, it is built by locating the upper and lower As atoms on the lower and upper S atoms, respectively.

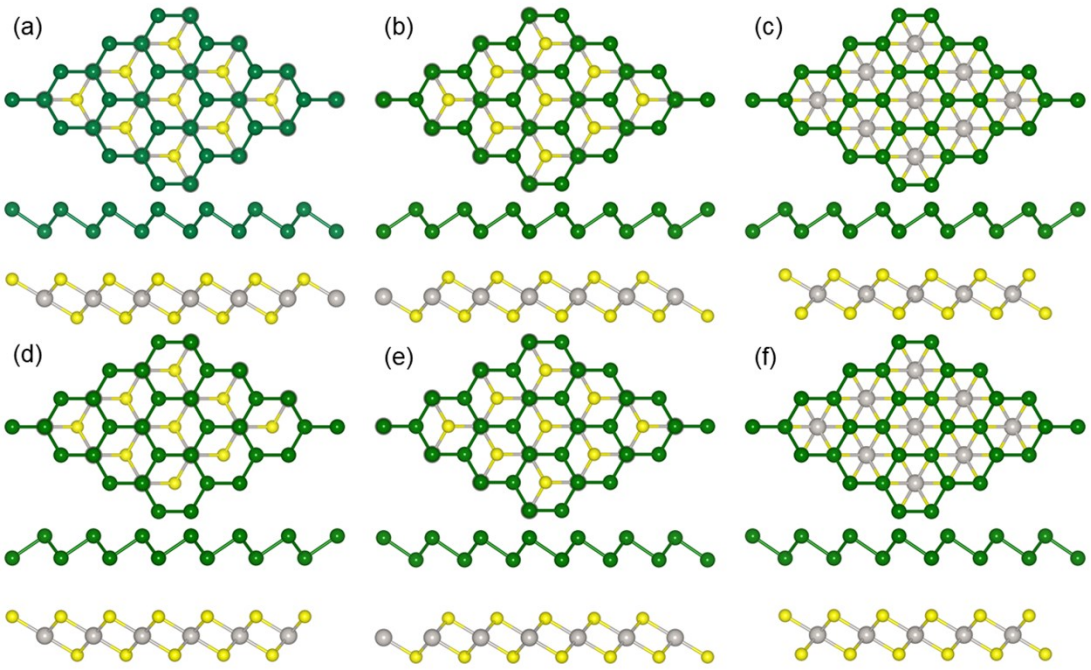

Fig. S2. Top and side views of the PtS_2/Are heterostructure for representative stacking: (a) stacking-A, (b)

stacking-B, (c) stacking-C, (d) stacking-D, (e) stacking-E and (f) stacking-F; the yellow, gray and green balls represent S, Pt and As atoms, respectively.

The binding energy, the interlayer distance and bond length of the different stacking configurations of the PtS_2/Are heterostructure are shown in Table S1. One can see that the stacking-C configuration of the PtS_2/Are heterostructure has the lowest binding energy of –14.814 meV/Å^2, showing the formation by weaken van der Waals forces [1]. The bond length of the Pt–S and As–As in the PtS_2 and Are monolayers are optimized by 2.398 and 2.506 Å, respectively. And the bond length of the Pt–S and As–As in the optimized PtS_2/Are heterostructure are 2.400 and 2.493 Å, respectively, which only slightly change compared with the pristine monolayer PtS_2 and Are, further demonstrating the formation of vdW heterostructure.

Table S1. Calculated binding energy (E_b) and the interlayer distance (d) and bond length ($B_{Pt–S}$ and $B_{As–As}$) of the different stacking configurations for the optimized PtS_2/Are heterostructure.

	stacking-A	stacking-B	stacking-C	stacking-D	stacking-E	stacking-F
E_b (meV/Å^2)	–13.104	–13.861	–14.814	–8.217	–14.495	–8.487
d (Å)	3.044	2.908	2.770	3.718	2.442	3.644
$B_{Pt–S}$ (Å)	2.398	2.402	2.400	2.399	2.391	2.497
$B_{As–As}$ (Å)	2.495	2.494	2.493	2.497	2.488	2.399

3. Effect of water molecule on stability of vdW heterostructure.

We also investigated the effect of water molecules (H_2O) on the stability of Are/PtS_2 vdW heterostructure by calculating the binding energy. We defined the H_2O adsorbed system heterostructure, PtS_2 and Are as PtS_2/Are(H_2O), PtS_2(H_2O) and Are(H_2O), respectively, as shown in Fig. S3. The binding energy between PtS_2 and Are layers can be obtained by:

$$E_{b(H2O)} = E_{Are/PtS2(H2O)} - E_{PtS2(H2O)} - E_{Are(H2O)}, \quad \text{(S1)}$$

where $E_{PtS2/Are(H2O)}$, $E_{PtS2(H2O)}$ and $E_{Are(H2O)}$ are the total energy of the H_2O adsorbed PtS_2/Are heterostructure, H_2O adsorbed PtS_2 and H_2O adsorbed Are systems, respectively. E_b is –26.395 meV/Å^2, which demonstrates the stability of the Are/PtS_2 vdW heterostructure.

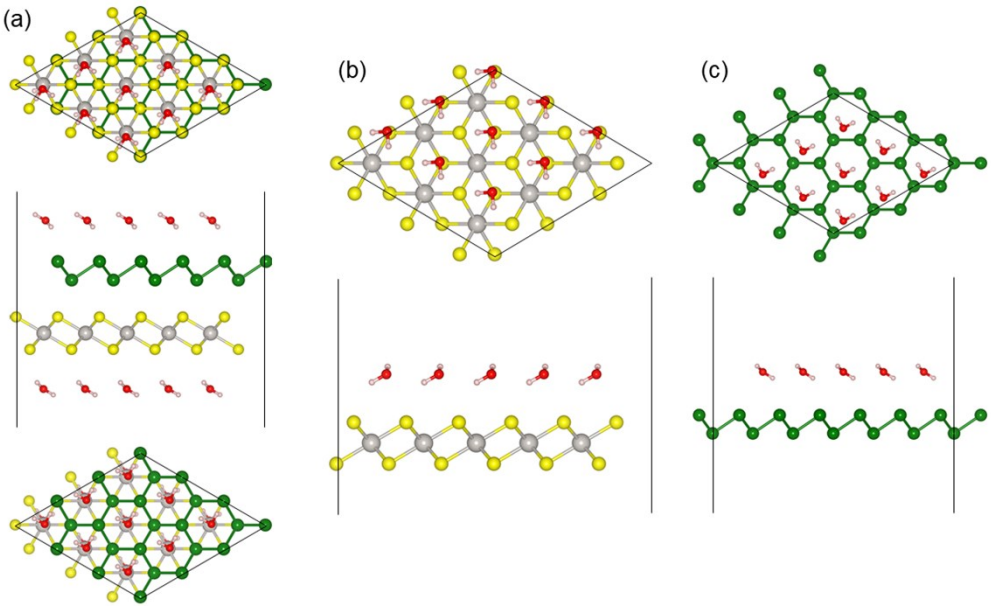

Fig. S3. (a) The H_2O adsorbed PtS_2/Are vdW heterostructure, (b) H_2O adsorbed PtS_2 and (c) H_2O adsorbed Are system. The yellow, gray and green, red and pink balls represent S, Pt, As, O and H atoms, respectively.

4. Exciton binding energy

The exciton binding energy (E_{eb}) can quantitatively evaluate the recombination rate of the photogenerated electron−hole pairs. The E_{eb} of the monolayer Are, PtS_2 and PtS_2/Are vdW heterostructure are calculated through Mott-Wannier hydrogenic model [S2]:

$$E_{eb} = \frac{13.6\mu_{ex}}{m_0 \varepsilon^2}, \ \mu_{ex} = \frac{m_e m_h}{m_e + m_h} \tag{S2}$$

where μ_{ex} is the effective exciton mass, and ε is the macroscopic static dielectric constant, which is the sum of electronic (ε_{el}) and ionic (ε_{ion}) contributions, respectively. The higher value of E_{eb} corresponds to the more difficult separation of the photogenerated electron-hole pairs. In Table S2, the E_{eb} of the PtS_2/Are vdW heterostructure is 0.47 eV, which is smaller than monolayer Are of 0.49 eV and PtS_2 of 1.34 eV. Therefore, the PtS_2/Are vdW heterostructure can remarkably improve the efficiency of the photocatalysis for water splitting, compared to the monolayer Are and PtS_2.

Table S2. The ε_{el}, ε_{ion} and E_{eb} of monolayer Are, PtS_2 and Are/PtS_2 vdW heterostructure.

	ε_{el}			ε_{ion}			E_{eb}
	x	y	z	x	y	z	
Are	0.02	0.02	0.03	3.97	3.97	1.20	0.49
PtS_2	0.02	0.02	0.01	3.97	3.97	1.18	1.34
Are/PtS_2	2.58	2.58	1.89	7.07	7.07	1.34	0.47

5. The band edge positions of the Are and PtS_2 monolayers

The band edge positions of the Are and PtS_2 monolayers are shown in Fig. S4. It is clear that both Are and PtS_2 monolayers possess decent potentials of the CBM and VBM for the reduction and oxidation reaction at pH=0. The overpotentials of $\chi(H_2)$ and $\chi(O_2)$ for Are and PtS_2 monolayers are 0.848 eV and 1.375 eV, respectively, which demonstrate the HER activity of Ars and OER activity of PtS_2.

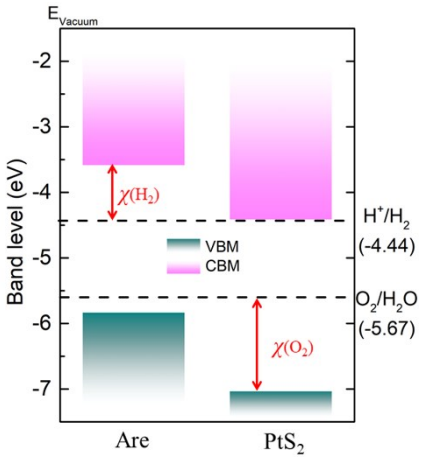

Fig. S4. The band alignment of the Are and PtS_2 monolayers with respect to the water oxidation (O_2/H_2O) and reduction (H^+/H_2) potentials at pH=0. All results are obtained by HSE06 functional calculation.

6. Optical absorption spectrum

Because most of the data in literature is obtained from HSE06 calculations, for a fair comparison, we also calculated the optical absorption of the PtS_2/Are vdW heterostructure with HSE06 functional. As shown in Fig. S5, in ultraviolet (UV) region, the absorption peaks of PtS_2, Are monolayers and PtS_2/Are vdW heterostructure are 5.404 × 10^5, 9.120 × 10^5 and 10.346 × 10^5 cm^{-1} located at the wavelength of 311.557, 232.768 and 245.652 nm, respectively. Meanwhile, near the visible light spectrum, the HSE06 functional calculated absorption peaks of PtS_2, Are monolayers and PtS_2/Are vdW heterostructure are 4.738 × 10^5, 2.495 × 10^5 and 4.594 × 10^5 cm^{-1}, respectively. The optical absorption ability of the PtS_2/Are vdW heterostructure is superior to other TMDs-based vdW heterostructures, such as TMDs/GeC (about 1.902–4.548 × 10^5 cm^{-1}) [S3], TMDs/BSe (about 0.451–1.715 × 10^5 cm^{-1}) [S4] and TMDs/$Mg(OH)_2$ (about 1.511–1.934 × 10^5 cm^{-1}) [S5] heterostructures.

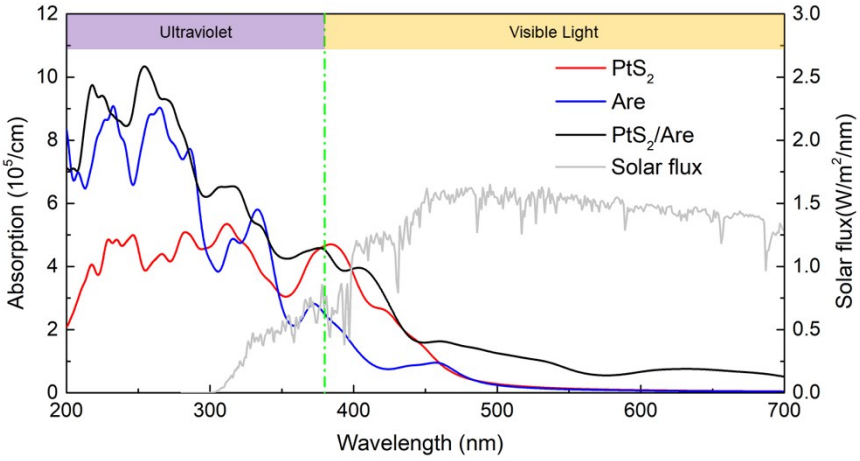

Fig. S5. The optical absorption spectrum of the monolayer PtS_2, Are and PtS_2/Are vdW heterostructure calculated by HSE06 functional.

References

[S1] X. Chen, F. Tian, C. Persson, W. Duan, N.X. Chen, Interlayer interactions in graphites, *Sci. Rep*., 3 (2013) 3046.

[S2] B. Ram, A.K. Singh, Strain-induced indirect-to-direct band-gap transition in bulk SnS_2, *Phys. Rev. B*, 95 (2017), 075134.

[S3] K. Ren, M. Sun, Y. Luo, S. Wang, Y. Xu, J. Yu, W. Tang, Electronic and optical properties of van der Waals vertical heterostructures based on two-dimensional transition metal dichalcogenides: First-principles calculations, *Phys. Lett. A*, 383 (2019) 1487–1492.

[S4] Y. Luo, K. Ren, S. Wang, J.-P. Chou, J. Yu, Z. Sun, M. Sun, First-Principles Study on Transition-Metal Dichalcogenide/BSe van der Waals Heterostructures: A Promising Water-Splitting Photocatalyst, *J. Phys. Chem. C*, 123 (2019) 22742–22751.

[S5] Y. Luo, S. Wang, K. Ren, J.P. Chou, J. Yu, Z. Sun, M. Sun, Transition-metal dichalcogenides/$Mg(OH)_2$ van der Waals heterostructures as promising water-splitting photocatalysts: a first-principles study, Phys Chem Chem Phys, 21 (2019) 1791–1796.